Title
Retinal Structure and Function in Achromatopsia Implications for Gene Therapy

Journal
Ophthalmology, 121(1)

ISSN
0161-6420

Authors
Sundaram, Venki
Wilde, Caroline
Aboshiha, Jonathan
et al.

Publication Date
2014

DOI
10.1016/j.ophtha.2013.08.017

Peer reviewed

Published in final edited form as:
Ophthalmology. 2014 January ; 121(1): 234–245. doi:10.1016/j.ophtha.2013.08.017.

Retinal Structure and Function in Achromatopsia: Implications for Gene Therapy

Venki Sundaram, FRCOphth[1,2], **Caroline Wilde, MBBS**[1], **Jonathan Aboshiha, MRCOphth**[1,2], **Jill Cowing, PhD**[1], **Colin Han**[3], **Christopher S. Langlo**[4], **Ravinder Chana, MSc**[1,2], **Alice E. Davidson, PhD**[1,2], **Panagiotis I. Sergouniotis, MD, PhD**[1], **James W. Bainbridge, PhD, FRCOphth**[1,2], **Robin R. Ali, PhD**[1], **Alfredo Dubra, PhD**[5,6], **Gary Rubin, PhD**[1], **Andrew R. Webster, MD, FRCOphth**[1,2], **Anthony T. Moore, FRCOphth**[1,2], **Marko Nardini, PhD**[1], **Joseph Carroll, PhD**[4,5,6,*], and **Michel Michaelides, MD, FRCOphth**[1,2,*]

[1]UCL Institute of Ophthalmology, University College London, London, UK

[2]Moorfields Eye Hospital, London, UK

[3]Summer Program for Undergraduate Research, Medical College of Wisconsin, Milwaukee, WI, USA

[4]Department of Cell Biology, Neurobiology & Anatomy, Medical College of Wisconsin, Milwaukee, WI, USA

[5]Department of Ophthalmology, Medical College of Wisconsin, Milwaukee, WI, USA

[6]Department of Biophysics, Medical College of Wisconsin, Milwaukee, WI, USA

Abstract

Purpose—To characterize retinal structure and function in achromatopsia (ACHM) in preparation for clinical trials of gene therapy.

Design—Cross-sectional study.

Participants—Forty subjects with ACHM.

Methods—All subjects underwent spectral domain optical coherence tomography (SD-OCT), microperimetry, and molecular genetic testing. Foveal structure on SD-OCT was graded into 5 distinct categories: (i) continuous inner segment ellipsoid (ISe), (ii) ISe disruption, (iii) ISe absence, (iv) presence of a hyporeflective zone (HRZ), and (v) outer retinal atrophy including retinal pigment epithelial (RPE) loss. Foveal and outer nuclear layer (ONL) thickness was measured, and presence of hypoplasia determined.

Main Outcome Measures—Photoreceptor appearance on SD-OCT imaging; foveal and ONL thickness; presence of foveal hypoplasia; retinal sensitivity and fixation stability; and association of these parameters with age and genotype.

[*]Joint Senior Authors and Authors for Correspondence: Dr Michel Michaelides, UCL Institute of Ophthalmology, 11-43 Bath Street, London, EC1V 9EL, UK, michel.michaelides@ucl.ac.uk; Professor Joseph Carroll Medical College of Wisconsin, Milwaukee, WI, USA jcarroll@mcw.edu.

There is no conflict of interest.

Results—Forty subjects with mean age of 24.9 years (range 6 to 52) were included. Disease-causing variants were found in *CNGA3* (n=18), *CNGB3* (n=15), *GNAT2* (n=4), and *PDE6C* (n=1). No variants were found in 2 individuals. 22.5% of subjects had a continuous ISe layer at the fovea; 27.5% had ISe disruption; 20% had an absent ISe layer; 22.5% had a HRZ; and 7.5% had outer retinal atrophy. No significant differences in age (p=0.77), mean retinal sensitivity (p=0.21) or fixation stability (p=0.34) across the 5 SD-OCT categories were evident. No significant correlation was found between age and foveal thickness (p=0.84), or between age and foveal ONL thickness (p=0.12).

Conclusions—The lack of clear association of disruption of retinal structure or function in ACHM with age suggests that the window of opportunity for intervention by gene therapy is wider in some individuals than previously indicated. Therefore the potential benefit for a given subject is likely to be better predicted by specific measurement of photoreceptor structure rather than simply by age. The ability to directly assess cone photoreceptor preservation with SD-OCT and/or adaptive optics imaging is likely to prove invaluable in selecting subjects for future trials and measuring their impact.

Introduction

Achromatopsia (ACHM) is a cone dysfunction syndrome with an incidence of approximately 1 in 30,000, which presents at birth or early infancy.[1] It is characterized by marked photophobia and nystagmus, reduced visual acuity (20/120 to 20/200), very poor or absent color vision, and absent cone electroretinogram (ERG) responses, with normal rod function. Fundus examination is usually normal, although retinal pigment epithelial (RPE) disturbance and atrophy may be present. Mutations in 5 genes have been identified in ACHM, *CNGA3*, *CNGB3*, *GNAT2*, *PDE6C* and *PDE6H* – all of which encode components of the cone phototransduction cascade.[2-5] *CNGA3* and *CNGB3* encode the α and β subunits of the cGMP gated cation channel respectively, and account for approximately 80% of cases of ACHM.[1,2] Sequence variants in *GNAT2*, *PDE6C* and *PDE6H* are uncommon causes of ACHM, each accounting for less than 2% of patients, and encode the α-subunit of transducin, and the α and γ subunits of cGMP phosphodiesterase respectively[3-5].

There have been several optical coherence tomography (OCT) based studies that have investigated outer retinal architecture and foveal morphology in ACHM.[6-9] The macular appearances described include normal lamination, variable degrees of disruption of the hyperreflective photoreceptor bands (known as either the inner segment (IS)/outer segment (OS) junction or inner segment ellipsoid (ISe)), an optically empty cavity or hyporeflective zone (HRZ), and complete outer retinal and RPE loss.[6-9] There are significant limitations to these studies, including the fact that subjects were not genotyped in all cases, and many relied on qualitative metrics to analyze the OCT images. In addition, there is conflicting data on progression and the presence or absence of age-dependent outer retinal loss, with Thiadens *et al*.[6] and Thomas *et al*. [7] suggesting age-associated progression, whereas Genead *et al*. provided evidence that cone loss is not age-dependent.[8] These inconsistencies and the fact that several groups around the world are in preparation for gene replacement clinical trials, makes it critical to elucidate the progressive nature (and thus the therapeutic window) in ACHM in a genotype-dependent fashion.

Several studies have shown that gene therapy can be effective in restoring cone function in multiple animal models of ACHM.[10-14] In a *Cngb3*$^{-/-}$ mouse model, subretinal gene delivery resulted in near normal restoration of electrophysiological function and significantly improved visual behaviour,[13] with larger canine models of *CNGB3*-associated disease also showing increased electrophysiological responses and improvements in navigational ability following gene replacement therapy.[14] In anticipation of the imminent human gene therapy trials for ACHM, we sought to characterize the relationship between

retinal structure and function in a large number of molecularly proven subjects. This information is important to help identify the most suitable candidates for therapy, to determine the optimal timing for intervention, and to measure its impact using appropriate outcome measures.

Methods

Subjects

Forty subjects with a clinical diagnosis of ACHM were included in this study. Ten additional subjects with normal vision were recruited. The protocol of the study adhered to the Tenets of the Declaration of Helsinki, was approved by the local Ethics Committees of Moorfields Eye Hospital and the Medical College of Wisconsin, and was performed with the informed consent of all subjects.

Clinical Assessments

All subjects underwent a clinical history and detailed ocular examination, including best-corrected visual acuity (BCVA) using an Early Treatment Diabetic Retinopathy Study (ETDRS) chart, reading acuity using the MNRead chart, contrast sensitivity assessment using the Pelli-Robson chart at 1m, color vision testing (Ishihara and Hardy Rand Rittler (HRR) pseudoisochromatic plates), color fundus photography, spectral domain OCT (SD-OCT), and microperimetry.

On the basis of their fundus appearance on color fundus photography, each subject was assigned to one of 3 categories: (i) no RPE disturbance, (ii) RPE disturbance, or (iii) atrophy.

Spectral Domain Optical Coherence Tomography (SD-OCT)

For all subjects (80 eyes of 40 subjects) following pupillary dilation, line and volume scans were obtained using a Spectralis® SD-OCT (Heidelberg Engineering, Heidelberg, Germany). The volume acquisition protocol consisted of 49 B-scans (124 microns between scans; 20×20°), with the Automatic Real Time (ART) eye tracking used when possible. The lateral scale of each image was estimated using the axial length data obtained from the Zeiss IOL Master.

Qualitative Assessment of Foveal Morphology—Foveal structure on SD-OCT images was graded into one of five categories (Figure 1): (i) continuous inner segment ellipsoid (ISe), (ii) ISe disruption, (iii) ISe absence, (iv) presence of a hyporeflective zone (HRZ), or (v) outer retinal atrophy, including RPE loss. The presence/absence of foveal hypoplasia was also noted, defined as the persistence of one or more inner retinal layers (outer plexiform layer, inner nuclear layer, inner plexiform layer or ganglion cell layer) through the fovea. Figure 2 shows examples of the varying degrees of foveal hypoplasia observed in the subjects examined herein. Consensus grading was established by three independent examiners (VS, JC and MM).

Quantitative Analysis of Photoreceptor Structure on SD-OCT—We used a method that was conceptually similar to the one described by Hood *et al*. to analyze the intensity of the ISe and ELM bands;[15] though there are a number of differences. Firstly, our images were transformed into a linear display using a transform provided by the manufacturer. This is a critical correction to apply, as the native visualization of OCT images on a logarithmic scale misrepresents the real differences in reflectivity (Figure 3). Secondly, we only assessed layer intensity at two specific retinal locations, 1mm and 1.5mm temporal to the fovea (due to the outer retinal disruption in many subjects, 1mm was the

closest eccentricity we could measure in all subjects). Finally, the procedure used to measure layer intensity was different. We generated longitudinal reflectivity profiles (LRP)[16] at the 1mm and 1.5mm locations, and each LRP was 5 pixels in width (Figure 3). Hood *et al*. defined a "local region" surrounding a specific segment of the ISe as extending ± 275μm to either side of the ISe segment and extending axially between the Bruch's membrane/choroid interface and the posterior border of the retinal nerve fiber layer (RNFL).[15] Since other posterior layers may be altered due to the disruption in cone structure, including the outer nuclear layer + Henle Fiber Layer (ONL+HFL), or the layers posterior to the ISe that are thought to originate from interactions between the photoreceptors and RPE,[17] we used a "local region" restricted to the retinal ganglion cell (RGC) layer and inner plexiform layer (IPL). This is indicated by the horizontal arrows in Figure 3. We then measured the peak image intensity at the ELM and ISe (labeled in Figure 3), and the relative intensity of the ISe (or ELM) was taken as the ISe (or ELM) peak intensity divided by the average intensity in the "local region".

In addition to examining the ELM and IS/OS intensity, we measured the total retinal thickness (ILM to RPE distance) and ONL thickness (posterior OPL boundary to ELM distance) at the fovea. In cases of foveal hypoplasia, the distance between the posterior OPL boundary and the ELM was taken as the ONL thickness. All thickness measurements were conducted by a single observer (CH) using ImageJ.

Microperimetry

Microperimetry (MP) was performed on both eyes of all subjects using the MP-1 microperimeter (Nidek Technologies, Padova, Italy). Specific details can be found in the on-line only material (Appendix 1, available at http://aaojournal.org).

Molecular Genetic Testing

Conventional direct Sanger sequencing of exons and exon-intron boundaries of *CNGA3, CNGB3, GNAT2* and *PDE6C* was undertaken using previously published methods.[2-4] Subjects 39 and 40 also underwent screening of exons and exon-intron boundaries of *PDE6H*[5].

Statistical Analysis

Normality of data was assessed by evaluating the shape of histogram plots, with age, BCVA, contrast sensitivity and reading acuity considered to be normally distributed. Inter-eye correlations for all parameters were assessed using Pearson or Spearman correlation analysis where appropriate. The left eye was arbitrarily selected for further analysis, and differences in parameters between OCT groups, fundus appearance category and genotype were assessed using the one-way analysis of variance (ANOVA) or Kruskal-Wallis test where appropriate. Differences in parameters between subjects with or without foveal hypoplasia were assessed using either an independent samples t-test, or Mann-Whitney U test where appropriate.

Results

Twenty male and 20 female subjects with a mean age of 24.9 years (range 6 to 52) were included (Tables 1 and 2). Mean BCVA was 0.92 logMAR (range 0.72 to 1.32), mean contrast sensitivity was 1.16 logCS (range 0.50 to 1.55), and mean reading acuity was 0.76 logMAR (range 0.5 to 1.32) (Table 2). There was no significant correlation between age and (i) BCVA (r=0.18, p=0.27, Figure 4), (ii) contrast sensitivity (r= −0.27, p=0.09), or (iii) reading acuity (r=0.29, p=0.07).

All subjects were able to read the Ishihara test plate, but were unable to read any subsequent plates, or correctly identify any of the HRR test plates.

Fundus examination revealed no evidence of macular retinal pigment epithelial (RPE) disturbance in 11 subjects (mean age 19.5 years; range 6-33), RPE disturbance in 20 subjects (mean age 27.5 years; range 12-52), and well-circumscribed macular atrophy in 9 subjects (mean age 25.9 years; range 11 to 43) (Table 2). There was no significant difference in mean age, BCVA, contrast sensitivity, reading acuity, retinal sensitivity or BCEA between these three groups (**Table 3**, available at http://aaojournal.org).

Molecular Genetics

Eighteen subjects (45%) had mutations in *CNGA3* (mean age 24.1 years; range 7-49), 15 (37.5%) had mutations in *CNGB3* (mean age 20.4 years; range 6-47), 4 (10%) had mutations in *GNAT2* (mean age 43.3 years; range 29-52), and 1 subject had a mutation in *PDE6C* (Tables 1, 2 and 4). Seven novel mutations were found in our group of 40 subjects (Table 4). No likely disease-associated variants were identified in 2 individuals, which included screening for *PDE6H* mutations, in addition to the above 4 genes. Detailed *in silico* analysis of both previously described and novel variants is shown in Table 4.[2, 19-22]

Foveal Morphology

On the basis of SD-OCT imaging, subjects were placed into one of five groups (Figure 1): (i) 9 subjects (22.5%) had a continuous inner segment ellipsoid (ISe) layer at the fovea (mean age 26.8 years; range 6 to 52); (ii) 11 (27.5%) had ISe disruption at the fovea (mean age 23.8 years; range 11 to 35); (iii) 8 (20%) had an absent ISe layer at the fovea (mean age 20.6 years; range 7 to 43); (iv) 9 (22.5%) had a foveal hyporeflective zone (HRZ) (mean age 28.2; range 11 to 49); and (v) 3 subjects (7.5%) had evidence of outer retinal atrophy at the fovea, including RPE loss (mean age 25 years; range 23 to 27) (**Table 5**, available at http://aaojournal.org). Out of the nine subjects with macular atrophy on fundus examination, three subjects were in OCT group 2, two in OCT group 3, one in OCT group 4, and three subjects in OCT group 5. The proportion of subjects with any disruption in cone structure (SD-OCT categories 2 to 5) was consistent with previous studies[6-8].

There were no significant differences in the age (p=0.77), BCVA (p=0.44), contrast sensitivity (p=0.57) or retinal sensitivity (p=0.21) between subjects in the five OCT categories; however reading acuity was significantly lower (p=0.02) in subjects with no ISe disruption compared to subjects with a HRZ (**Table 5**, available at http://aaojournal.org). Figure 5 shows representative SD-OCT images of subjects of different ages and genotypes; illustrating the variable appearances within different genotypes and the lack of age-dependence on the integrity of outer retinal architecture.

Foveal hypoplasia was found in 21 (52.5%) subjects (Table 1; and **Table 6**, available at http://aaojournal.org); with it not being possible to assess hypoplasia in 2 subjects due to severe foveal atrophy. Our rate of hypoplasia was slightly lower than two previous reports, which used different definitions of hypoplasia than that used herein.[6,7] There was no significant difference in age, contrast sensitivity, retinal sensitivity or fixation stability between subjects with or without foveal hypoplasia. Surprisingly, BCVA (p<0.01) and reading acuity (p<0.01) were better in subjects with evidence of foveal hypoplasia compared to those without (**Table 6**, available at http://aaojournal.org).

External Limiting Membrane (ELM) and Inner Segment Ellipsoid (ISe) Relative Intensity

The mean intensity ratios of the ISe band, measured at 1mm and 1.5mm from the fovea in the 40 ACHM subjects, were 2.66 (range 1.4 to 5.3) and 2.90 (range 1.12 to 9.06),

respectively (Table 1). These intensities were significantly lower compared to 10 controls with mean ISe intensity of 6.16 (range 4.18 to 9.25, p<0.001) at 1mm from the fovea, and 6.65 at 1.5mm (range 3.93 to 10.88, p<0.001) from the fovea; although there was overlap between the range of intensities observed in ACHM subjects and controls.

In contrast, the mean intensity ratios of the ELM band, measured at 1mm and 1.5mm from the fovea in the 40 ACHM subjects, were 0.66 (range 0.32 to 1.40) and 0.68 (range 0.35 to 1.18), respectively (Table 1). These intensities were similar to those measured in 10 controls, with mean ELM intensity ratios of 0.69 (range 0.39 to 1.01, p=0.45) at 1mm from the fovea, and 0.60 at 1.5mm (range 0.39 to 0.84, p=0.57) from the fovea.

No significant differences were found in ELM or ISe intensity ratios between *CNGA3* and *CNGB3* subjects, with the mean ELM intensity ratios at 1mm and 1.5mm from the fovea being 0.66 and 0.71 in *CNGA3* subjects, and 0.67 and 0.67 in *CNGB3* subjects, respectively (p=0.42, and p=0.80). The mean ISe intensity ratios at 1mm and 1.5mm from the fovea were 2.54 and 2.59 in *CNGA3* subjects, and 2.48 and 2.58 in *CNGB3* subjects, respectively (p=0.61, and p=0.37).

Foveal Outer Nuclear Layer and Total Retinal Thickness

Mean foveal thickness and ONL thickness at the fovea in ACHM subjects were 163.6μm (range 62.0 to 313.2μm) and 67.1μm (range 26.2 to 110.5μm), respectively, which were significantly lower than mean foveal thickness (190.4μm, range 136.2 to 217.0, p=0.02) and mean ONL thickness at the fovea (104.9μm, range 82.9 to 119.5, p=<0.001) in controls. Again, it is worth noting that there was overlap between the ACHM subjects and controls, consistent with the presence of retained cone nuclei in some ACHM subjects. No significant correlation was found between age and either foveal thickness (ρ=0.03, p=0.84) or foveal ONL thickness (ρ=0.26, p=0.12) in subjects with ACHM.

Microperimetry

All 40 subjects underwent microperimetry testing on at least two occasions. There was no significant difference in mean retinal sensitivity and fixation stability between eyes, and further analysis was therefore performed using the left eye only in each subject. No significant difference in mean retinal sensitivity or fixation stability was found between subjects' first and second test; the mean of these two tests was used for subsequent analysis.

The mean retinal sensitivity of the group was 16.6 dB (range 3.1 to 19.9 dB), and the mean fixation stability of the group was 13.5° (range 1.7 to 65°); with significant negative correlations found between retinal sensitivity and (i) age (ρ= −0.39, p=0.01, Figure 6), (ii) BCVA (ρ= −0.44, p<0.01, Figure 7), and (iii) reading acuity (ρ= −0.55, p<0.01). Surprisingly, a significant correlation was found between lower contrast sensitivity and both higher retinal sensitivity (ρ=0.35, p=0.03) and higher fixation stability (ρ= −0.43, p<0.01). There was no significant difference in mean retinal sensitivity (p=0.21) or fixation stability (p=0.34) across the 5 OCT groups (**Table 5**, available at http://aaojournal.org). There was a significant correlation between fixation stability and BCVA (ρ=0.43, p<0.01).

Six subjects had a scotoma (0 dB sensitivity in ≥ 1 location), with a mean sensitivity in this group of 11.0 dB (range 3.1 to 14.8 dB), and mean fixation stability of 12.8° (range 1.7° to 24°). The mean age of these subjects was 40.2 years (range 25 to 52 years), and mean BCVA was 1.01 logMAR (range 0.8 to 1.32). Four of these 6 subjects had RPE disturbance on fundus examination, with the remaining 2 subjects having macular atrophy. It is of note that variable macular structure was seen on SD-OCT, with 3 of the 6 subjects having a

normal ISe layer, and 1 subject each having an absent foveal ISe layer, or HRZ, or outer retinal atrophy.

Genotype-Phenotype Correlation

The vast majority (82.5%) of subjects in our study had either *CNGA3* or *CNGB3* mutations. There were no significant differences between the subjects with these two genotypes in terms of age, BCVA, contrast sensitivity, reading acuity, or fixation stability (**Table 7**, available at http://aaojournal.org). However, retinal sensitivity was significantly greater in the *CNGB3* group than in the *CNGA3* group (18.1dB compared to 16.1dB, p=0.04).

A comparison of the SD-OCT phenotypes and presence of foveal hypoplasia failed to identify any consistent differences between the *CNGA3* and *CNGB3* subjects. Specifically, 26.7% (n=4) of subjects with *CNGB3* mutations had no ISe disruption, compared to 11.1% (n=2) with *CNGA3* variants; and (20%, n=3) subjects harboring *CNGB3* variants had ISe disruption compared to 44.4% (n=8) in the *CNGA3* group (**Table 7**, available at http://aaojournal.org). The presence of an HRZ was similar in *CNGA3* (n=4, 22.5%) and *CNGB3* (n=4, 26.7%) subjects. Outer retinal atrophy was observed in 13.3 % (n=2) of *CNGB3* subjects compared to 5.5% (n=1) of *CNGA3* subjects. In the *CNGA3* group, 61% (n=11) of subjects had foveal hypoplasia, compared to 53% (n=8) of *CNGB3* subjects. Foveal hypoplasia was not present in the 4 subjects with *GNAT2* mutations, or in the single *PDE6C* subject.

On examination, 44.4% (n=7) of *CNGA3* subjects had a normal fundus appearance, compared to 20% (n=3) in the *CNGB3* group, and 33.3% (n=6) of *CNGA3* subjects had RPE disturbance compared to 53% (n=8) of subjects with *CNGB3* variants. The percentage of subjects with macular atrophy was similar in both groups (*CNGA3* 22.3%, n=4; *CNGB3* 27%, n=4). Of the 6 subjects with a scotoma on microperimetry, 4 individuals had *GNAT2* variants, 1 had *PDE6C* variants and 1 had *CNGA3* variants. In addition, BCVA, contrast sensitivity, reading acuity and mean sensitivity were lower in the *GNAT2* and *PDE6C* genotypes, compared to the *CNGA3* or *CNGB3* groups; however the mean age of subjects with either *GNAT2* or *PDE6C* mutations was considerably higher than the *CNGA3*/*CNGB3* group (**Table 7**, available at http://aaojournal.org). Interestingly, 3 out of the 4 subjects with *GNAT2* mutations had an intact ISe layer, despite a relatively low mean retinal sensitivity of 13.6dB, with all of these subjects having a central scotoma on microperimetry.

Discussion

Lack of Age-Dependence of Cone Loss

Our cross-sectional study (n=40) identified no age-dependent loss of cone structure in subjects with ACHM. For example, we found that cone loss (SD-OCT categories 3 to 5) was evident in approximately 57% (16/28) of subjects less than 30 years of age, but in only 33% (4/12) aged over 30 years. Moreover, subjects without ISe disruption (most preserved cone structure) had the second highest mean age of the five OCT categories, and no reduction in ISe intensity was found with advancing age. In addition, foveal ONL and total retinal thickness was significantly reduced, though we did not find an association between retinal thinning and advancing age. In contrast to our findings, Thiadens *et al*. reported that cone loss occurred in 42% (8/19) of affected individuals who were under 30 years of age, with 95% (20/21) over 30 years showing cone loss on SD-OCT.[6] Thomas *et al*. also reported age-dependent ONL thinning.[7] One possible explanation for this discrepancy is the lack of standardization of how cone loss is measured. Moving forward it will be important to conduct larger studies with molecularly proven subjects in which the same anatomical measures are undertaken.

Whilst our study demonstrates that outer retinal changes do not necessarily occur in a predictable age-dependent manner, a recent small (n=8) longitudinal study observed progressive changes in retinal morphology in younger but not older patients.[23] However, bearing in mind the characteristic phenotypic variability of inherited retinal disease, longitudinal studies are needed to examine the progressive nature of ACHM. It is important to note that progression does not imply that age alone should be a principal eligibility criterion for emerging trials; in other words different patients likely progress at different rates.

Retinal Function

We identified no significant correlation of deterioration in BCVA, contrast sensitivity or reading acuity with advancing age, and to the best of our knowledge, this is the largest study to date reporting on any potential change in these parameters with age. We did, however, find a decline in microperimetry-based retinal sensitivity with age. A significant reduction in retinal sensitivity, determined by mesopic microperimetry, has been reported to occur in normal subjects with increasing age, with a 1dB lower retinal sensitivity found in subjects aged 70 to 75 years compared to those aged 20 to 29 years.[24] In our study the decline in sensitivity of 3.1dB observed between subjects less than 25 years of age (n=22) and those over 25 years (n=18), is greater than that potentially attributable to age-related decline.

In our cohort of subjects with absent cone function (on the basis of electrophysiology and psychophysics), it is presumed that retinal sensitivity detected by mesopic microperimetry testing is a consequence of retained rod function. This raises the question as to whether rod function declines in subjects with ACHM with age and if so, why? If there is no change in rod function, it remains a possibility that there is residual central cone function in some subjects, which may deteriorate over time. Further investigation is required to determine which class of photoreceptor(s) is responsible for the retinal sensitivity detected by mesopic microperimetry in ACHM; for example by measuring the rate of recovery of retinal sensitivity using the aforementioned microperimeter following a full bleach might help to shed light on this intriguing issue.

Structure-Function Relationships

We identified no clear association between retinal structure and function, with no differences in BCVA, contrast sensitivity, retinal sensitivity or fixation stability between subjects with the various SD-OCT findings or fundus changes. This is in keeping with the lack of an association reported between the presence of an HRZ and visual acuity in previous studies.[6,7] Surprisingly, subjects without ISe disruption had a significantly ($p=0.02$) lower reading acuity compared to subjects with HRZ presence - however, a statistical difference was not found in any other functional parameter, suggesting this is not a clinically significant observation. No correlation was found between ISe intensity and retinal sensitivity, although this is perhaps to be expected, as in the absence of cone function, retinal sensitivity is likely to be primarily derived from rod function in ACHM subjects.

We found no significant differences in contrast sensitivity, retinal sensitivity or fixation stability in subjects with or without foveal hypoplasia; however, surprisingly, significantly better BCVA and reading acuity were found in subjects with foveal hypoplasia. This is reminiscent of findings in albinism, where the absence of a fovea does not necessarily impair acuity.[25,26] However, a structural grading system for foveal hypoplasia reported by Thomas *et al*. has suggested a relationship between foveal development and acuity.[27] It is also likely that varying degrees of nystagmus amplitude or frequency between subjects contribute to determining BCVA and retinal sensitivity in ACHM and other disorders.

Implications for Gene Therapy

Gene replacement trials for both *CNGA3* and *CNGB3* are planned in the near future. Our findings of no age-dependence of cone loss demonstrate that the potential window of opportunity for therapeutic intervention in ACHM is wider than has previously been suggested; subjects with no evidence of ISe disruption were aged between 6 and 52 years and we found no correlation of cone photoreceptor disruption or loss with increasing age.

As this was a cross-sectional study, it has not assessed whether subjects who have any form of outer retinal change develop progressive degeneration, and if so, how variable the rate of change may be. With respect to cone photoreceptor structure, we therefore suggest that candidates should be considered for potential gene therapy intervention on an individual basis, irrespective of their age. In addition, we did not observe decreased visual function in subjects with foveal hypoplasia; in fact significantly better BCVA and reading acuity were found in subjects with foveal hypoplasia, suggesting that foveal hypoplasia per se should not be an exclusion criterion for potential therapy trials. In the 9 subjects with no ISe disruption evident on SD-OCT, their mean ISe intensity ratio was considerably lower than in healthy controls, illustrating that assessment of the degree of residual cone structure using this metric may be useful in determining the suitability of potential trial participants. However, direct visualization of the cone mosaic is afforded through the use of adaptive optics imaging.[28-30] There is a need to elucidate the relationship between these various measures of cone structure in ACHM to establish the most appropriate means to identify suitable patients and track therapeutic efficacy.

In addition to cone photoreceptor integrity, another factor likely to influence the response to gene therapy is the ability of the visual system to respond to newly acquired input. Functional magnetic resonance imaging has shown evidence of visual cortex reorganization in ACHM subjects, with the area of visual cortex normally active following cone-derived foveal stimulation, being active instead following rod stimuli.[31] Conversely, recovery of cone-driven cortical activity has been observed in a canine model of ACHM (Gingras G. Cortical recovery following gene therapy in a canine model of achromatopsia. Paper presented at: The Vision Sciences Society Meeting, May 8, 2009; Florida). The extent to which the visual cortex is able to adapt to and process new input from cone photoreceptors is an additional consideration likely to influence the efficacy of gene replacement therapy.

Supplementary Material

Refer to Web version on PubMed Central for supplementary material.

Acknowledgments

The work was supported by grants from the National Institute for Health Research Biomedical Research Centre at Moorfields Eye Hospital NHS Foundation Trust and UCL Institute of Ophthalmology, Fight For Sight, Moorfields Eye Hospital Special Trustees, The Wellcome Trust, Retinitis Pigmentosa Fighting Blindness, and the Foundation Fighting Blindness (USA). MM is supported by a Foundation Fighting Blindness Career Development Award. JWB is a NIHR Research Professor. MCW Funding: NIH grants R01EY017607, P30EY001931, C06RR016511, Foundation Fighting Blindness, and an unrestricted departmental grant from Research to Prevent Blindness (RPB). AD is the recipient of a Burroughs Wellcome Fund Career Award at the Scientific interface and a Career Development Award from RPB.

Appendix 1: Microperimetry

Microperimetry (MP) was performed on both eyes of all subjects using the MP-1 microperimeter (Nidek Technologies, Padova, Italy). Test-retest variability was investigated by all subjects having 2 tests undertaken on each eye. A customized test grid of 44 retinal

locations with an eight degree radius was used to cover the macular and para-macular region; with a mean retinal sensitivity recorded over this test area. Testing was conducted in a darkened room and all subjects underwent training at the beginning of the MP session to ensure correct operation of the response trigger, immediately prior to formal testing. All tests were performed after pupil dilatation with tropicamide 1% and phenylephrine 2.5%. The contralateral (non-tested) eye was occluded.

Subjects were instructed to fixate on a 2-degree cross fixation target and background illuminance was set within the mesopic range at 1.27cd/m^2. A Goldmann size III stimulus with an area of 4mm^2 and 200ms duration was used. A 4-2 testing strategy was employed, with the intensity of the stimulus reduced in 4dB steps until it is no longer recognized by the subject. The threshold is then crossed a second time by increasing the stimulus intensity by 2dB steps until it is detected once again. False positive errors were tested for by measuring responses to stimuli projected into the blind spot at 30 second intervals. Fixation stability was assessed using the bivariate contour ellipse area (BCEA) which represents an area in degrees where 68% of fixation points are located;[18] this value is reported by the Nidek software. An active eye tracking system corrects for fixation errors to ensure accurate stimulus projection in relation to retinal landmarks.

Repeat testing was performed on all subjects using the “follow-up” test option, which requires alignment of specific retinal landmarks at each subsequent test, to ensure similar location of stimuli projection.

References

1. Michaelides M, Hunt DM, Moore AT. The cone dysfunction syndromes. Br J Ophthalmol. 2004; 88:291–7. [PubMed: 14736794]
2. Johnson S, Michaelides M, Aligianis IA, et al. Achromatopsia caused by novel mutations in both *CNGA3* and *CNGB3* [report online]. J Med Genet. 2004; 41:e20. Available at: http://jmg.bmj.com/content/41/2/e20.long. [PubMed: 14757870]
3. Kohl S, Baumann B, Rosenberg T, et al. Mutations in the cone photoreceptor G-protein alpha-subunit gene *GNAT2* in patients with achromatopsia. Am J Hum Genet. 2002; 71:422–5. [PubMed: 12077706]
4. Thiadens AA, denHollander AI, Roosing S, et al. Homozygosity mapping reveals *PDE6C* mutations in patients with early-onset cone photoreceptor disorders. Am J Hum Genet. 2009; 85:240–7. [PubMed: 19615668]
5. Kohl S, Coppieters F, Meire F, et al. European Retinal Disease Consortium. A nonsense mutation in *PDE6H* causes autosomal-recessive incomplete achromatopsia. Am J Hum Genet. 2012; 91:527–32. [PubMed: 22901948]
6. Thiadens AA, Somervuo V, vandenBorn LI, et al. Progressive loss of cones in achromatopsia: an imaging study using spectral-domain optical coherence tomography. Invest Ophthalmol Vis Sci. 2010; 51:5952–7. [PubMed: 20574029]
7. Thomas MG, Kumar A, Kohl S, et al. High-resolution in vivo imaging in achromatopsia. Ophthalmology. 2011; 118:882–7. [PubMed: 21211844]
8. Genead MA, Fishman GA, Rha J, et al. Photoreceptor structure and function in patients with congenital achromatopsia. Invest Ophthalmol Vis Sci. 2011; 52:7298–308. [PubMed: 21778272]
9. Proudlock F, Gottlob I. Foveal development and nystagmus. Ann N Y Acad Sci. 2011; 1233:292–7. [PubMed: 21951007]
10. Alexander JJ, Umino Y, Everhart D, et al. Restoration of cone vision in a mouse model of achromatopsia. Nat Med. 2007; 13:685–7. [PubMed: 17515894]
11. Michalakis S, Muhlfriedel R, Tanimoto N, et al. Restoration of cone vision in the *CNGA3*-/- mouse model of congenital complete lack of cone photoreceptor function. Mol Ther. 2010; 18:2057–63. [PubMed: 20628362]

12. Pang JJ, Alexander J, Lei B, et al. Achromatopsia as a potential candidate for gene therapy. Adv Exp Med Biol. 2010; 664:639–46. [PubMed: 20238068]
13. Carvalho LS, Xu J, Pearson RA, et al. Long-term and age-dependent restoration of visual function in a mouse model of CNGB3-associated achromatopsia following gene therapy. Hum Mol Genet. 2011; 20:3161–75. [PubMed: 21576125]
14. Komaromy AM, Alexander JJ, Rowlan JS, et al. Gene therapy rescues cone function in congenital achromatopsia. Hum Mol Genet. 2010; 19:2581–93. [PubMed: 20378608]
15. Hood DC, Zhang X, Ramachandran R, et al. The inner segment/outer segment border seen on optical coherence tomography is less intense in patients with diminished cone function. Invest Ophthalmol Vis Sci. 2011; 52:9703–9. [PubMed: 22110066]
16. Huang Y, Cideciyan AV, Papastergiou GI, et al. Relation of optical coherence tomography to microanatomy in normal and *rd* chickens. Invest Ophthalmol Vis Sci. 1998; 39:2405–16. [PubMed: 9804149]
17. Spaide RF, Curcio CA. Anatomical correlates to the bands seen in the outer retina by optical coherence tomography: literature review and model. Retina. 2011; 31:1609–19. [PubMed: 21844839]
18. Crossland MD, Dunbar HM, Rubin GS. Fixation stability measurement using the MP1 microperimeter. Retina. 2009; 29:651–6. [PubMed: 19262440]
19. Kohl S, Marx T, Giddings I, et al. Total colourblindness is caused by mutations in the gene encoding the alpha-subunit of the cone photoreceptor cGMP-gated cation channel. Nat Genet. 1998; 19:257–9. [PubMed: 9662398]
20. Wissinger B, Gamer D, Jägle H, et al. *CNGA3* mutations in hereditary cone photoreceptor disorders. Am J Hum Genet. 2001; 69:722–37. [PubMed: 11536077]
21. Kohl S, Baumann B, Broghammer M, et al. Mutations in the *CNGB3* gene encoding the beta-subunit of the cone photoreceptor cGMP-gated channel are responsible for achromatopsia (*ACHM3*) linked to chromosome 8q21. Hum Mol Genet. 2000; 9:2107–16. [PubMed: 10958649]
22. Aligianis IA, Forshew T, Johnson S, et al. Mapping of a novel locus for achromatopsia (*ACHM4*) to 1p and identification of a germline mutation in the alpha subunit of cone transducin (*GNAT2*). J Med Genet. 2002; 39:656–60. [PubMed: 12205108]
23. Thomas MG, McLean RJ, Kohl S, et al. Early signs of longitudinal progressive cone photoreceptor degeneration in achromatopsia. Br J Ophthalmol. 2012; 96:1232–6. [PubMed: 22790432]
24. Midena E, Vujosevic S, Cavarzeran F. Microperimetry Study Group. Normal values for fundus perimetry with the microperimeter MP1. Ophthalmology. 2010; 117:1571–6. [PubMed: 20472294]
25. Marmor MF, Choi SS, Zawadzki RJ, Werner JS. Visual insignificance of the foveal pit: reassessment of foveal hypoplasia as fovea plana. Arch Ophthalmol. 2008; 126:907–13. [PubMed: 18625935]
26. McAllister JT, Dubis AM, Tait DM, et al. Arrested development: high-resolution imaging of foveal morphology in albinism. Vision Res. 2010; 50:810–7. [PubMed: 20149815]
27. Thomas MG, Kumar A, Mohammad S, et al. Structural grading of foveal hypoplasia using spectral-domain optical coherence tomography: a predictor of visual acuity? Ophthalmology. 2011; 118:1653–60. [PubMed: 21529956]
28. Merino D, Duncan JL, Tiruveedhula P, Roorda A. Observation of cone and rod photoreceptors in normal subjects and patients using a new generation adaptive optics scanning laser ophthalmoscope. Biomed Opt Express [serial online]. 2011; 2:2189–201. Available at: http://www.opticsinfobase.org/boe/fulltext.cfm?uri=boe-2-8-2392&id=220600.
29. Dubra A, Sulai Y, Norris JL, et al. Noninvasive imaging of the human rod photoreceptor mosaic using a confocal adaptive optics scanning ophthalmoscope. Biomed Opt Express [serial online]. 2011; 2:1864–76. Available at: http://www.opticsinfobase.org/boe/fulltext.cfm?uri=boe-2-7-1864&id=217386.
30. Carroll J, Dubra A, Gardner JC, et al. The effect of cone opsin mutations on retinal structure and the integrity of the photoreceptor mosaic. Invest Ophthalmol Vis Sci. 2012; 53:8006–15. [PubMed: 23139274]
31. Baseler HA, Brewer AA, Sharpe LT, et al. Reorganization of human cortical maps caused by inherited photoreceptor abnormalities. Nat Neurosci. 2002; 5:364–70. [PubMed: 11914722]

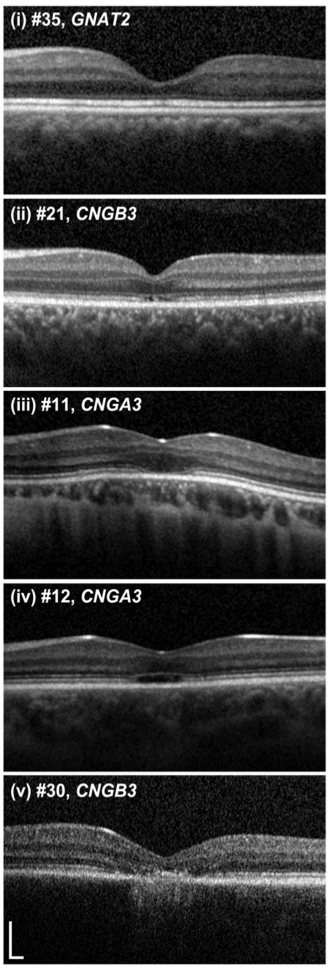

Figure 1. Representative images of the five optical coherence tomography phenotypes
Subjects were graded into one of five categories, (i)=continuous inner segment ellipsoid band (ISe); (ii)=ISe disruption; (iii)=ISe absence; (iv)=hyporeflective zone present; (v)=outer retinal atrophy. Scale bar is 200 microns.

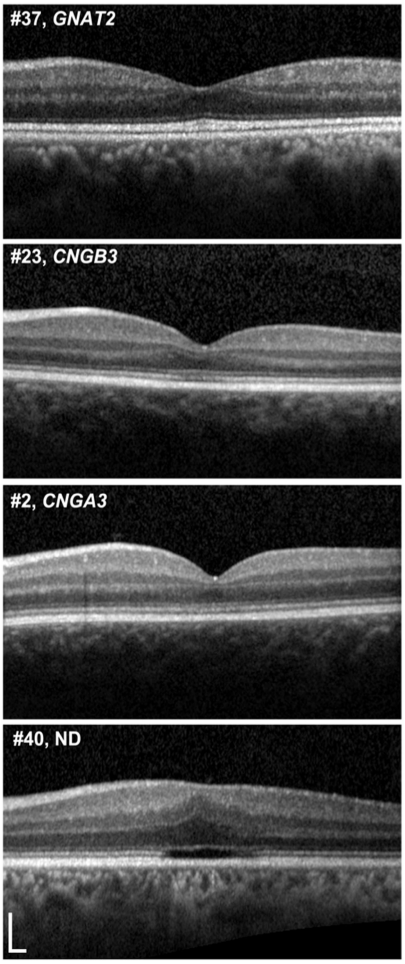

Figure 2. Representative examples of varying degrees of foveal hypoplasia

Foveal hypoplasia was defined here as the persistence of one or more inner retinal layers (outer plexiform layer, inner nuclear layer, inner plexiform layer or ganglion cell layer) through the foveal center. Normal retinal anatomy (top panel) shows complete excavation of the inner retinal layers at the fovea, resulting in the characteristic “pit”. However in a number of conditions (such as retinopathy of prematurity and albinism), this process is impaired (‘foveal hypoplasia’), resulting in retinas in which the inner retinal layers persist at the fovea. Interestingly this can also be seen in achromatopsia. The 3 lower panels show examples of varying degrees of foveal hypoplasia in patients with achromatopsia, in whom the fovea contains inner retinal layers as opposed to complete excavation of these layers. Twenty-one of the 40 subjects (52.5%) had foveal hypoplasia, though it was not possible to assess hypoplasia in 2 subjects due to severe foveal atrophy. There was no significant difference in age, contrast sensitivity, retinal sensitivity or fixation stability between subjects with or without foveal hypoplasia (see text). Scale bar is 200 microns. ND=no data.

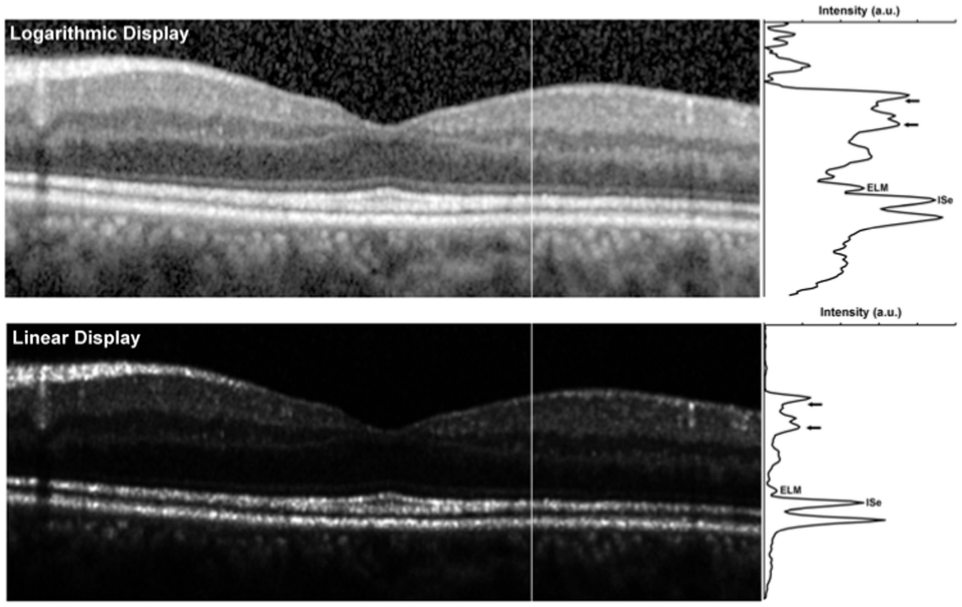

Figure 3. Longitudinal reflectivity profile assessment of photoreceptor integrity on SD-OCT

The top image is the native display of the image from the SD-OCT, while the lower image is a linear display of the actual image intensity. Note that in the linear (i.e. raw) OCT image, larger differences in layer intensity get compressed when visualized on a logarithmic display. Moreover the logarithmic transform will increase the widths of the hyperreflective bands being measured.[17] This highlights the need to use raw OCT data when making quantitative measures of layer intensity. Vertical lines in each image indicate the location of the longitudinal reflectivity profile (LRP) shown to the right of each image. SD-OCT=Spectral Domain Optical Coherence Tomography. OCT=Optical Coherence Tomography. ELM=external limiting membrane, ISe = inner segment ellipsoid. Short horizontal arrows define the boundaries of the "local region" used to normalize the ISe or ELM intensity. a.u. = arbitrary units.

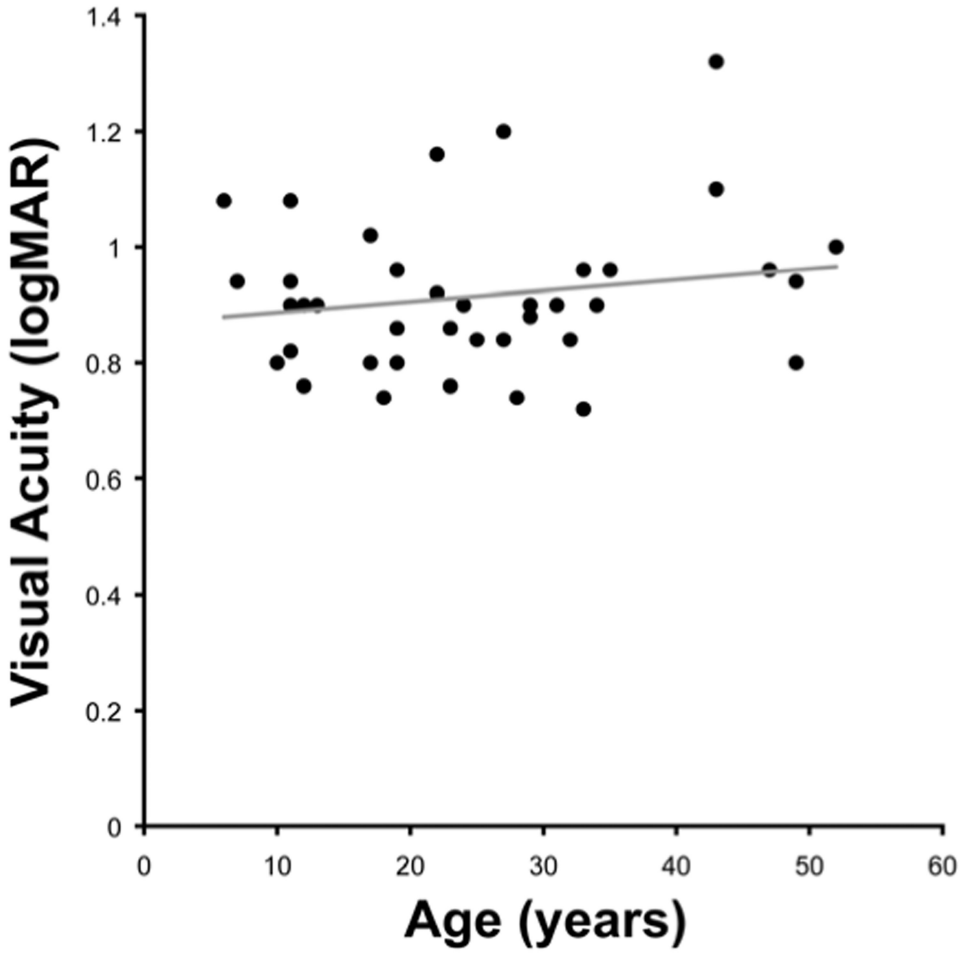

Figure 4. No significant decline in visual acuity as a function of age

Forty subjects with a mean age of 24.9 years (range 6 to 52) were included in this study, with a mean visual acuity of 0.92 (range 0.72 to 1.32). There was no significant correlation between age and visual acuity (r=0.18, p=0.27). Acuity reported as log minimum angle of resolution (logMAR).

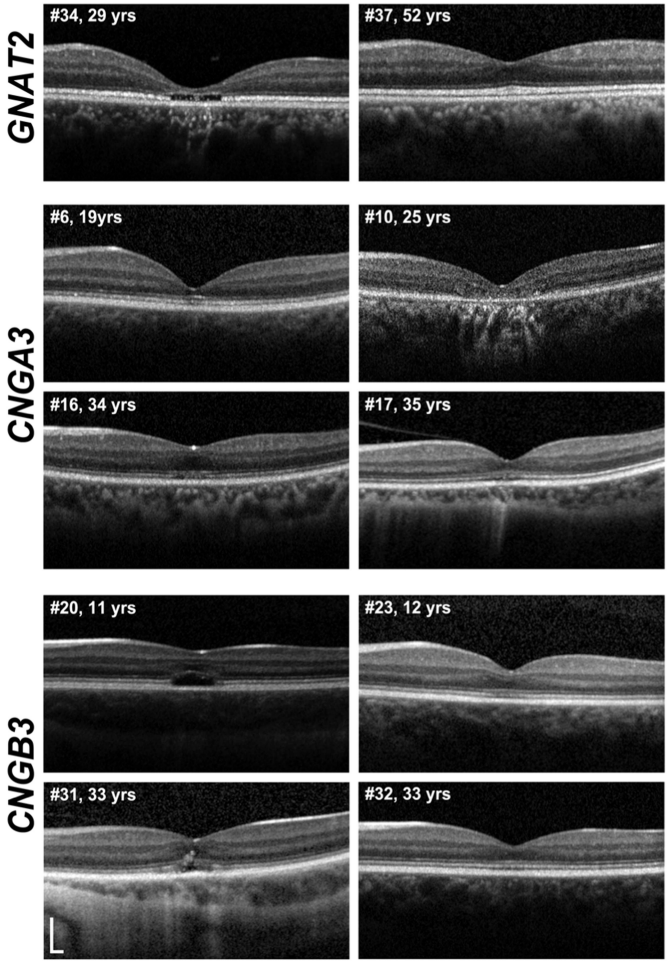

Figure 5. Variable SD-OCT appearance in subjects of various ages and genotypes

Representative SD-OCT images of subjects of different ages and genotypes; illustrating the variable appearances within different genotypes and the lack of age-dependence on the integrity of outer retinal architecture. Yrs=years. SD-OCT=Spectral Domain Optical Coherence Tomography.

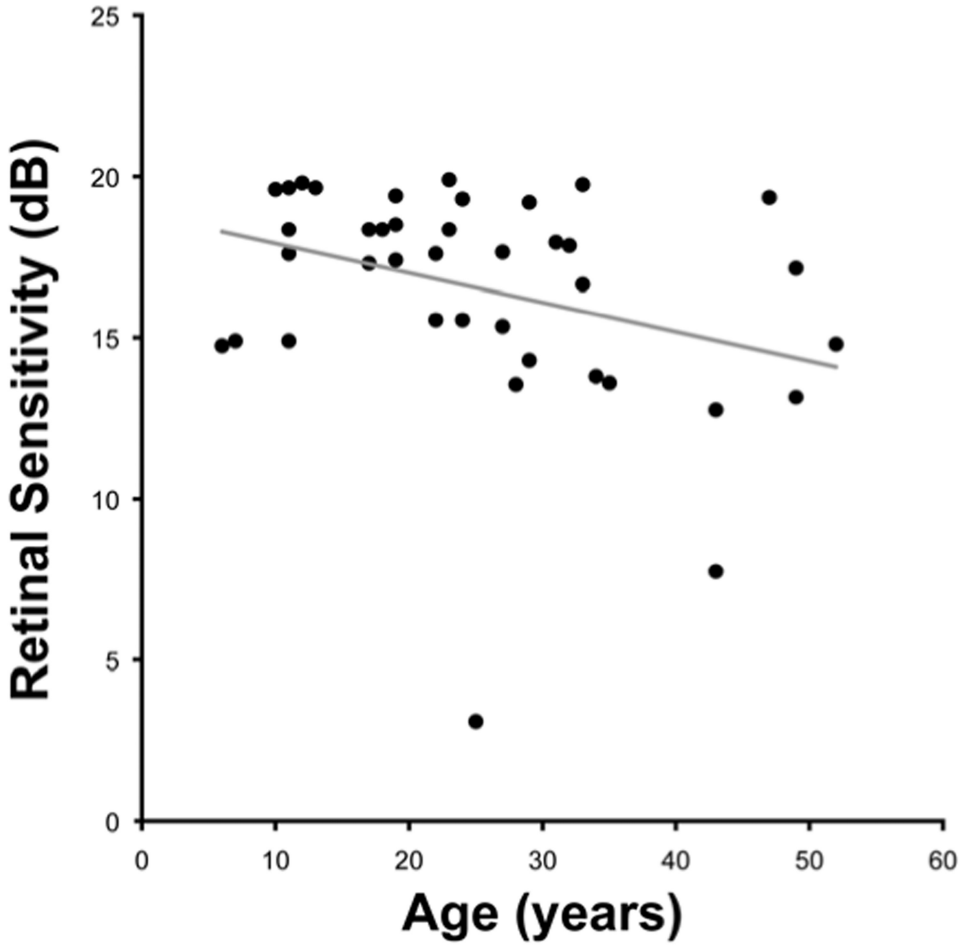

Figure 6. Negative correlation between age and retinal sensitivity

All 40 subjects underwent microperimetry testing on at least two occasions. There was no significant difference in mean retinal sensitivity between both eyes, and further analysis was therefore performed using the left eye only. No significant difference in mean retinal sensitivity was found between subjects' first and second test, and the mean of these two tests was used for subsequent analysis. The mean retinal sensitivity of the group was 16.6 dB (range 3.1 to 19.9 dB); with significant negative correlation found between retinal sensitivity and age ($\rho = -0.39$, $p=0.01$). Acuity reported as log minimum angle of resolution (logMAR).

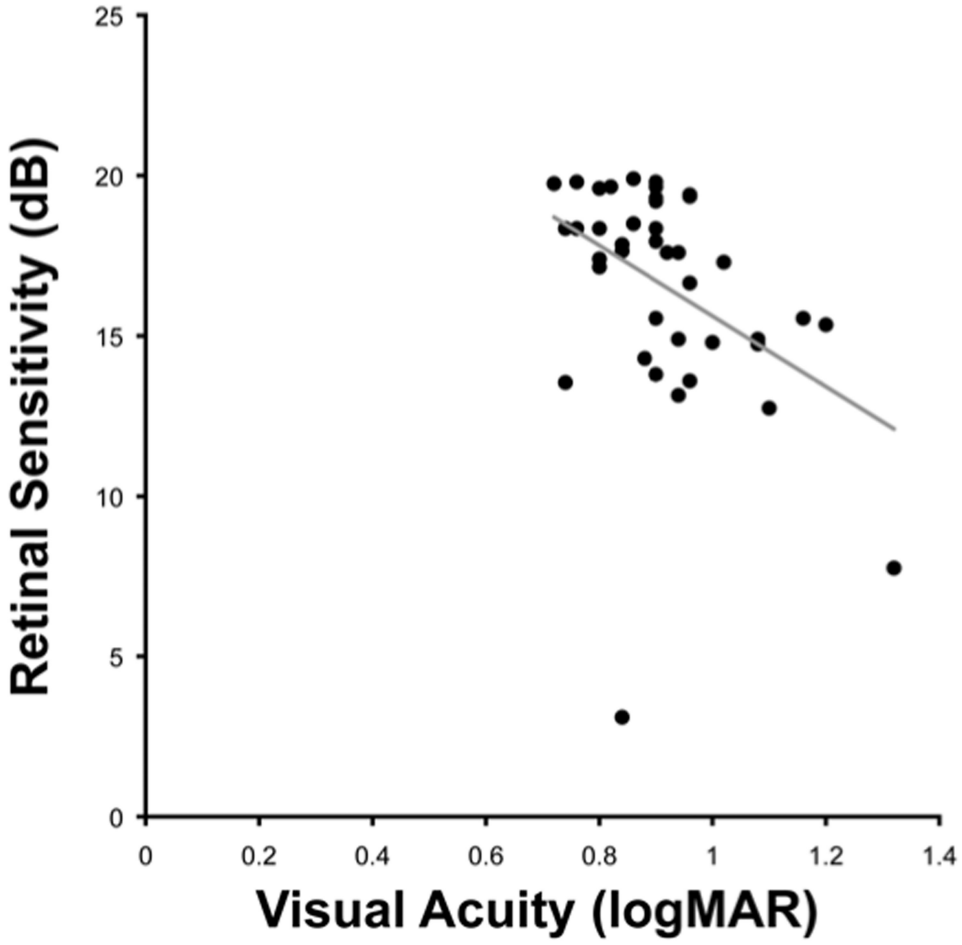

Figure 7. Negative correlation between visual acuity and retinal sensitivity

The mean retinal sensitivity of the cohort was 16.6 dB (range 3.1 to 19.9 dB); with significant negative correlation found between retinal sensitivity and visual acuity ($\rho = -0.44$, $p<0.01$). logMAR=log minimum angle of resolution.

Table 1

Summary of Retinal Structure Assessed with SD-OCT in 40 Patients with Achromatopsia

Patient Number	Age (y)	Sex	Axial Length (mm)	Gene	Allele 1/Allele 2	OCT Grade[δ]	Foveal Hypoplasia[δ]	ELM Ratio[‡]		ISe Ratio[‡]	
								1 mm	1.5 mm	1 mm	1.5 mm
1	7	M	23.93	*CNGA3*	c.1641C>A-p.Phe547Leu/c.1641C>A-p.Phe547Leu	3	Y	0.32	0.41	1.2	1.16
2	10	M	21.27	*CNGA3*	c.1642G>A-p.Gly548Arg/c.67C>T-p.Arg23Ter	1	Y	0.43	0.38	1.2	1.22
3	11	M	23.43	*CNGA3*	c.485A>T-p.Asp162Val/c.485A>T-p.Asp162Val	1	N	0.75	1.18	1.52	1.71
4	11	F	21.25	*CNGA3*	c.536T>A-p.Val179Asp/c.536T>A-p.Val179Asp	2	N	0.79	1.12	1.19	1.53
5	17	M	22.74	*CNGA3*	c.1001C>T-p.Ser334Phe/c.1360A>T-p.Lys454Ter	3	Y	0.66	0.57	1.68	1.09
6	19	F	22.49	*CNGA3*	c.1694C>T-p.Thr565Met/c.661C>T-p.Arg221Ter	2	N	0.83	0.57	2.25	2.26
7	22	F	23.96	*CNGA3*	c.847C>T-p.Arg283Trp/c.1279C>T-p.Arg427Cys	2	N	0.62	0.92	1.63	1.04
8	22	F	24.58	*CNGA3*	c.848G>A-p.Arg283Gln/c.667C>T-p.Arg223Trp	4	Y	0.66	0.64	1.66	1.73
9	24	M	24.57	*CNGA3*	c.848G>A-p.Arg283Gln/c.667C>T-p.Arg223Trp	2	Y	0.94	0.65	1.88	2
10	25	F	22.77	*CNGA3*	c.1315C>T-p.Arg439Trp/c.1315C>T-p.Arg439Trp	5	N/A	0.76	1.03	1.32	2.24
11	27	F	29.26	*CNGA3*	c.661C>T-p.Arg221Ter/c.661C>T-p.Arg221Ter	3	Y	0.76	0.55	2.33	2.41
12	28	F	25.51	*CNGA3*	c.848G>A-p.Arg283Gln/c.667C>T-p.Arg223Trp	4	Y	0.76	0.79	1.73	1.61
13	29	F	22.40	*CNGA3*	c.661C>T-p.Arg221Ter/c.848G>A-p.Arg283Gln	2	N	0.64	0.88	1.11	2.67
14	31	M	23.18	*CNGA3*	c.848G>A-p.Arg283Gln/c.667C>T-p.Arg223Trp	4	Y	0.54	0.77	1.74	1.59
15	32	F	25.52	*CNGA3*	c.1641C>A-p.Phe547Leu/c.1641C>A-p.Phe547Leu	2	Y	0.61	0.42	1.75	1.15
16	34	F	24.38	*CNGA3*	c.1443-1444insC-p.Ile482His fs*6/c.1706G>A-p.Arg569His	2	Y	0.55	0.56	1.02	1.21
17	35	M	28.06	*CNGA3*	c.661C>T-p.Arg221Ter/c.848G>A-p.Arg282Gln	2	N	0.52	0.61	1.99	2.67
18	49	F	24.90	*CNGA3*	c.67C>T-p.Arg23Ter/c.67C>T-p.Arg23Ter	4	Y	0.69	0.64	1.84	1.27
19	6	M	21.02	*CNGB3*	c.1148delC-p.Thr383Ile fs*13/c.1578+1G>A - Splice defect	1	N	0.51	0.73	0.83	1.08
20	11	M	23.63	*CNGB3*	c.1148delC-p.Thr383Ile fs*13/c.1148delC-p.Thr383Ile fs*13	4	Y	0.73	1.05	1.73	2.06
21	11	F	21.21	*CNGB3*	c.595delG-p.Glu199Ser fs*3/c.1148delC-p.Thr383Ile fs*13	2	Y	0.57	0.56	1.28	1.73
22	12	F	23.28	*CNGB3*	c.1148delC-p.Thr383Ile fs*13/c.1006G>T-p.Glu336Ter	3	Y	0.93	0.83	2.07	1.75
23	12	F	22.24	*CNGB3*	c.1148delC-p.Thr383Ile fs*13/c.1148delC-p.Thr383Ile fs*13	2	Y	0.6	0.49	1.61	1.52
24	13	M	23.42	*CNGB3*	c.595delG-p.Glu199Ser fs*3/c.1148delC-p.Thr383Ile fs*13	1	N	0.44	0.35	1.28	1.19
25	17	F	22.41	*CNGB3*	c.1148delC-p.Thr383Ile fs*13/c.1148delC-p.Thr383Ile fs*13	3	N	0.82	0.76	1.16	1.11
26	18	M	23.51	*CNGB3*	c.595delG-p.Glu199Ser fs*3/c.1148delC-p.Thr383Ile fs*13	4	Y	0.65	0.86	2.04	1.47
27	19	M	22.41	*CNGB3*	c.1148delC-p.Thr383Ile fs*13/c.1148delC-p.Thr383Ile fs*13	4	Y	1.4	0.57	1.96	1.01

Patient Number	Age (y)	Sex	Axial Length (mm)	Gene	Allele 1/Allele 2	OCT Grade[§]	Foveal Hypoplasia[δ]	ELM Ratio[‡]		ISe Ratio[‡]	
								1 mm	1.5 mm	1 mm	1.5 mm
28	23	M	23.67	*CNGB3*	c.1148delC-p.Thr383Ile fs*13/c.1148delC-p.Thr383Ile fs*13	5	Y	0.62	0.54	1.55	1.59
29	24	M	22.65	*CNGB3*	c.1148delC-p.Thr383Ile fs*13/c.607-608insT-p.Arg203Leu fs*3	1	N	0.54	0.57	0.8	0.67
30	27	M	22.85	*CNGB3*	c.1148delC-p.Thr383Ile fs*13/c.1853delC-p.Thr618Ile fs*2	5	N/A	0.48	0.43	2.23	3.91
31	33	F	25.91	*CNGB3*	c.1148delC-p.Thr383Ile fs*13/c.1148delC-p.Thr383Ile fs*13	2	Y	0.53	0.66	1.12	1.26
32	33	F	20.80	*CNGB3*	c.1148delC-p.Thr383Ile fs*13/c.1148delC-p.Thr383Ile fs*13	1	N	0.44	0.89	2.18	1.32
33	47	M	24.13	*CNGB3*	c.1148delC-p.Thr383Ile fs*13/c.1148delC-p.Thr383Ile fs*13	4	N	0.76	0.81	2.34	1.7
34	29	M	22.94	*GNAT2*	c.843-844insAGTC-p.His282Ser fs*11/c.843-844insAGTC-p.His282Ser fs*11	4	N	0.98	0.93	4.65	4.96
35	43	M	23.55	*GNAT2*	c.843-844insAGTC-p.His282Ser fs*11/c.843-844insAGTC-p.His282Ser fs*11	1	N	0.74	0.5	2.68	3.15
36	49	F	23.41	*GNAT2*	c.843-844insAGTC-p.His282Ser fs*11/c.843-844insAGTC-p.His282Ser fs*11	1	N	0.65	0.46	3.47	3.61
37	52	M	24.61	*GNAT2*	c.843-844insAGTC-p.His282Ser fs*11/c.843-844insAGTC-p.His282Ser fs*11	1	N	0.58	0.64	1.99	2.57
38	43	M	27.45	*PDE6C*	c.304C>T-p.Arg102Trp/c.304C>T-p.Arg102Trp	3	N	0.58	0.87	0.93	2.01
39	19	F	22.28	?	ND	3	Y	0.47	0.55	1.29	1.04
40	23	F	23.05	?	ND	3	Y	0.5	0.48	1.01	1.45

y=years, M=male, F=female, SD-OCT=spectral domain optical coherence tomography, ND=no mutation detected. The cDNA is numbered according to Ensembl transcript ID: CNGA3 ENST00000409933; CNGB3 ENST00000320005; GNAT2 ENST00000351050; PDE6C ENST00000371447, in which +1 is the A of the translation start codon.

[§]1=continuous ISe; 2=ISe disruption; 3=ISe absence; 4=hyporeflective zone; 5=outer retinal atrophy;

[δ]N/A = not possible to assess due to presence of outer retinal atrophy;

[‡]ELM=external limiting membrane, ISe=inner segment ellipsoid.

Table 2

Summary of Clinical Characteristics.

Variable	Mean (SD)	Range	Median
Age (years)	24.9 (12.3)	6-52	23.5
Visual acuity (logMAR)	0.92 (0.13)	0.72-1.32	0.9
Contrast sensitivity (logCS)	1.16 (0.23)	0.50-1.55	1.2
Reading acuity (logMAR)	0.76 (0.19)	0.50-1.32	0.73
Retinal sensitivity (dB)	16.6 (3.4)	3.1-19.9	17.6
BCEA (degrees)	13.5 (13.5)	1.7-65	7.7
Genotype	**N (%)**		
CNGA3	18 (45)		
CNGB3	15 (37.5)		
GNAT2	4 (10)		
PDE6C	1 (2.5)		
Unknown	2 (5)		
OCT category	**N (%)**		
1	9 (22.5)		
2	11 (27.5)		
3	8 (20)		
4	9 (22.5)		
5	3 (7.5)		
Foveal hypoplasia	**N (%)**		
No	17 (42.5)		
Yes	21 (52.5)		
Unrecordable	2 (5)		
Fundus appearance category	**N (%)**		
1	11 (28)		
2	20 (50)		
3	9 (22)		

OCT category: 1=continuous ISe; 2=ISe disruption; 3=ISe absence; 4=Hyporeflective zone present; 5=Outer retinal atrophy. Fundus appearance category: 1=no RPE disturbance; 2=RPE disturbance; 3=Atrophy present.

logMAR = logarithm of the minimum angle of resolution; logCS = logarithm of contrast sensitivity; SD = standard deviation; dB = decibel; BCEA = bivariate contour ellipse area; OCT = optical coherence tomography; ISe = inner segment ellipsoid; RPE = retinal pigment epithelium.

Table 4

Summary of Potentially Disease Associated Nonsynonymous Sequence Variants Identified in *CNGA3, CNGB3, GNAT2* and *PDE6C*

Gene	Nucleotide Alteration	Protein Alteration	Alleles	EVS Observed Allele Count	SIFT Tolerance Index (0-1)	PoyPhen2 HumVar Score (0-1)	Blosum 62 Score (4-11)	Disease Causing	Previously Reported
CNGA3	c.848G>A	p.Arg283Gln	6	A=2/G=10756	DAMAGING 0.02	PRD 0.996	-1	Yes	Kohl *et al*. 1998[19]
CNGA3	c.661C>T	p.Arg221Ter	5	ND	NA	NA	NA	Yes	Johnson *et al.* 2004[2]
CNGA3	c.667C>T	p.Arg223Trp	4	ND	DAMAGING 0.00	PRD 1.000	-3	Yes	Wissinger *et al*. 2001[20]
CNGA3	c.1641C>A	p.Phe547Leu	4	ND	DAMAGING 0.05	PRD 0.999	0	Yes	Kohl *et al*. 1998[19]
CNGA3	c.67C>T	p.Arg23Ter	3	ND	NA	NA	NA	Yes	Johnson *et al.* 2004[2]
CNGA3	c.485A>T	p.Asp162Val	2	ND	TOLERATED 0.6	POS 0.908	-3	Possibly	Wissinger *et al*. 2001[20]
CNGA3	c.536T>A	p.Val179Asp	2	ND	DAMAGING 0.00	PRD 0.941	-3	Yes	This Study
CNGA3	c.1315C>T	p.Arg439Trp	2	ND	DAMAGING 0.01	POS 0.901	-3	Yes	This Study
CNGA3	c.1642G>A	p.Gly548Arg	1	ND	DAMAGNG 0.00	PRD 1.000	-2	Yes	Johnson *et al.* 2004[2]
CNGA3	c.847C>T	p.Arg283Trp	1	T=1/C=10757	DAMAGING 0.00	PRD 1.000	-3	Yes	Kohl *et al*. 1998[19]
CNGA3	c.1001C>T	p.Ser334Phe	1	ND	TOLERATED 1.00	POS 0.744	-2	Possibly	This Study
CNGA3	c.1694C>T	p.Thr565Met	1	T=2/C=13004	DAMAGING 0.03	PRD 0.999	-1	Yes	Wissinger *et al*. 2001[20]
CNGA3	c.1360A>T	p.Lys454Ter	1	ND	NA	NA	NA	Yes	This Study
CNGA3	c.1279C>T	p.Arg427Cys	1	T=10/C=10748	DAMAGING 0.00	PRD 1.000	-3	Yes	Wissinger *et al*. 2001[20]
CNGA3	c.1706G>A	p.Arg569His	1	A=1/G=13005	DAMAGING 0.00	PRD 0.991	0	Yes	Wissinger *et al*. 2001[20]
CNGA3	c.1443-1444insC	p.Ile482His fs*6	1	ND	NA	NA	NA	Yes	Johnson *et al.* 2004[2]
CNGB3	c.1148delC	p.Thr383Ile fs*13	23	ND	NA	NA	NA	Yes	Kohl *et al*. 2000[21]
CNGB3	c.595delG	p.Glu199Ser fs*3	3	ND	NA	NA	NA	Yes	Johnson *et al.* 2004[2]
CNGB3	c.1006G>T	p.Glu336Ter	1	ND	NA	NA	NA	Yes	Kohl *et al*. 2000[21]
CNGB3	c.607-608insT	p.Arg203Leu fs*3	1	ND	NA	NA	NA	Yes	This Study
CNGB3	c.1853delC	p.Thr618Ile fs*2	1	ND	NA	NA	NA	Yes	This Study
CNGB3	c.1578+1 G>A	Splice defect	1	ND	NA	NA	NA	Yes	Kohl *et al*. 2000[21]
GNAT2	c.843-844insAGTC	p.His282Ser fs*11	8	ND	NA	NA	NA	Yes	Aligianis *et al*. 2002[22]
PDE6C	c.304C>T	p.Arg102Trp	2	ND	DAMAGING 0.00	PRD 0.999	-3	Yes	This Study

NA = not applicable, ND = not detected, POS =possibly damaging, PRD = probably damaging.

The predicted biological effect of nonsynonymous variants identified in *CNGA3, CNGB3, GNAT2 and PDE6C* were scored for likely pathogenicity using EVS, SIFT, PolyPhen2 and Blosum62. EVS denotes variants in the Exome Variant Server, NHLBI Exome Sequencing Project, Seattle, WA, USA. (http://snp.gs.washington.edu/EVS/, accessed April, 2013). SIFT (version 4.0.4 http://sift.jcvi.org/, accessed April, 2013) results are reported to be tolerated if tolerance index ≥ 0.05 or damaging if tolerance index < 0.05. Polyphen-2 (version 2.1 http://genetics.bwh.harvard.edu/pph2/, accessed April, 2013) appraises mutations qualitatively as Benign, Possibly Damaging (POS) or Probably Damaging (PRD) based on the model's false positive rate. In the Blosum62 (http://www.ncbi.nlm.nih.gov/Class/FieldGuide/BLOSUM62.txt, accessed April, 2013) substitution matrix score, positive numbers indicate a substitution more likely to be tolerated evolutionarily and negative numbers suggest the opposite. The cDNA is numbered according to Ensembl transcript ID: CNGA3 ENST00000409937; CNGB3 ENST00000320005; GNAT2 ENST00000351050; PDE6C ENST00000371447, in which +1 is the A of the translation start codon. Mutations in the coding region of each gene and at intron-exon boundaries are identified.